Research Square

Preprints are preliminary reports that have not undergone peer review.
They should not be considered conclusive, used to inform clinical practice,
or referenced by the media as validated information.

# Sentinel Plants Enable Aboveground Detection of Belowground Soil Microbial Activity

**Gozde Demirer**

gdemirer@caltech.edu

California Institute of Technology https://orcid.org/0000-0002-3007-1489

**Yunqing Wang**

Caltech

**John Marken**

California Institute of Technology

**Eugene Li**

Caltech

**Paul Tarr**

California Institute of Technology

**Chiara Berruto**

California Institute of Technology

**Elliot Meyerowitz**

California Institute of Technology https://orcid.org/0000-0003-4798-5153

**Article**

**Keywords:** Rhizosphere, plant-microbe communication, synthetic biology, cross-kingdom signaling, biosensors, sentinel plants, phytosensors, pC-HSL

**Posted Date:** April 17th, 2026

**DOI:** https://doi.org/10.21203/rs.3.rs-9256612/v1

**License:** This work is licensed under a Creative Commons Attribution 4.0 International License.
Read Full License

**Additional Declarations:** There is **NO** Competing Interest.

# Sentinel Plants Enable Aboveground Detection of Belowground Soil Microbial Activity

Yunqing Wang[1], John P. Marken[1], Eugene Li[2], Paul T. Tarr[3], Chiara Berruto[1], Elliot M. Meyerowitz[3], Gozde S. Demirer[2,#]

[1] Biology and Biological Engineering Division, California Institute of Technology, Pasadena, CA, USA
[2] Chemistry and Chemical Engineering Division, California Institute of Technology, Pasadena, CA, USA
[3] Howard Hughes Medical Institute and Biology and Biological Engineering Division, California Institute of Technology, Pasadena, CA, USA

# corresponding author: gdemirer@caltech.edu

## Abstract

Rhizosphere microbial processes play a central role in soil function and plant health yet remain difficult to monitor noninvasively and continuously. Engineered plants that detect microbially produced signals offer a scalable approach. However, existing systems have been limited to root-localized reporter readouts. Here, we optimize a synthetic p-coumaroyl-homoserine lactone (pC-HSL)-responsive circuit in *Arabidopsis thaliana* to enable aboveground reporting of belowground microbial activity. Sentinel plants detect root-applied pC-HSL at concentrations as low as 30 nM with a 25-fold increase in reporter expression in roots and a 270-fold increase in leaf fluorescence at 3 μM pC-HSL, demonstrating long-distance signal relay from roots to shoots. Moreover, sentinel plants report pC-HSL produced by engineered *Escherichia coli* and *Pseudomonas putida* at the root zone in both agar plate and agricultural soil assays. This work establishes a generalizable platform that enables plants to convert belowground microbial signals into visible aboveground readouts for noninvasive monitoring of rhizosphere microbial activity.

**Keywords:** Rhizosphere; plant-microbe communication; synthetic biology; cross-kingdom signaling; biosensors; sentinel plants; phytosensors; pC-HSL

## Introduction

The rhizosphere, a narrow zone of soil directly influenced by plant roots, is an essential component of soil health and agricultural sustainability, where microbial communities drive nutrient cycling, affect greenhouse gas emissions, and shape crop productivity[1]. Despite this key ecological importance, microbial activity in the rhizosphere remains difficult to monitor because existing methods rely on destructive sampling or indirect chemical measurements that lack sufficient spatiotemporal resolution[2]. Sensing approaches that do not perturb and can resolve underground microbial activity could advance the study and management of soil health for global sustainability[3].

Among emerging strategies for rhizosphere monitoring, microbial biosensors couple soil inputs to quantifiable outputs. These systems consist of genetically engineered bacteria that integrate input-responsive transcriptional regulators with optical or electrochemical reporters, thereby forming programmable input-output circuits[2]. Such biosensors have been developed to detect nutrient availability and pollutants[4–6]. Despite their versatility, deployment of microbial biosensors in open soil environments is constrained by containment challenges, regulatory uncertainty, and reliance on specialized instrumentation for signal readout. Spatial resolution is further constrained by the small, heterogeneous microenvironments that individual microbes sample, though hyperspectral imaging may partially address this limitation at the field scale[7].

Plants offer an alternative chassis for environmental biosensing. Unlike microbial biosensors, plants inherently integrate and transmit signals from the rhizosphere to aboveground tissues. They are self-powered via photosynthesis, and their capacity to generate diverse outputs, including pigments, scents, and volatile organic compounds, can enable detection at scale without specialized instrumentation[8]. Plants have been engineered to report a wide range of stressors, including osmotic stress, γ-radiation, fungicides and insecticides, and explosives such as trinitrotoluene[9–12]. Beyond abiotic stress, sentinel plants have been developed to detect biotic stressors, where field trials with engineered tobacco expressing a fluorescent protein under the control of synthetic salicylic acid-responsive promoters provided early warnings of pathogen infection[13]. In parallel, commercial efforts have begun to translate these concepts into agricultural applications. InnerPlant created an engineered soybean that fluoresces upon fungal infection, and Insignum developed maize that accumulates anthocyanins in response to fungal challenge[14,15].

Building on these advances, recent work has explored plants' ability to sense microbially produced molecules. Boo et al. established a cross-kingdom signaling system by engineering *Pseudomonas putida* and *Klebsiella pneumoniae* that produce *p*-coumaroyl-homoserine lactone (pC-HSL), which was detected by a synthetic circuit in plant roots[16]. pC-HSL is orthogonal to endogenous plant signaling pathways[17], genetically encodable in diverse microbial hosts[18,19], and detectable by a known receptor, making it a well-suited molecule for cross-kingdom communication. This work showed that plants can be engineered to respond to microbially synthesized signals. However, detection was limited to root-localized responses, and aboveground reporting of microbial signals has not yet been achieved, a requirement for scalable, noninvasive monitoring in soil.

Here, we optimize a pC-HSL-responsive synthetic circuit and generate *Arabidopsis thaliana* sentinel plants that sensitively detect microbially synthesized pC-HSL and convert it into a visible aboveground signal in both plate and soil environments. This work demonstrates that plants can perceive a bacterially produced signaling molecule and report this information in aboveground tissues, enabling a noninvasive readout of rhizosphere microbial gene expression. More broadly, this direct communication channel between rhizosphere microbes and plant leaves provides a framework for continuous, field-deployable monitoring of soil microbial function in agricultural and environmental settings.

## Results

### *pC-HSL-inducible circuit is optimized in transient Nicotiana benthamiana assays*

To establish a sentinel plant with high detection sensitivity and dynamic range, we first optimized a pC-HSL-inducible genetic circuit. This involved optimizing both the nuclear localization of the transcriptional activator RpaR, which binds pC-HSL and dimerizes, and the repeat number of its cognate operator sequence RpaO. We constructed a library of circuit variants by systematically altering the number of RpaO operator sites (0x, 2x, 4x, or 6x) upstream of the reporter gene (**Fig. 1A**). In parallel, we tested alternative nuclear localization signals (SV40 or bipartite BP) to modulate the strength of RpaR-VP16 nuclear import[20].

To account for batch-to-batch and plant-to-plant variability, we quantified reporter activity using a dual-luciferase assay. Green-enhanced Nano-lantern (GeNL) served as the inducible reporter, normalized to a constitutively expressed NanoLuc (Nluc)[21,22]. We expressed each construct in *N. benthamiana* leaves via *Agrobacterium*-mediated infiltration, and we treated the leaves with 0 to 10 µM pC-HSL after 48 h (**Supplementary Fig. 1A**).

Circuits containing six operator sites upstream of a minimal 35S promoter exhibited the largest fold change to pC-HSL (**Fig. 1B**). Dose-response analysis of the BP NLS-linked transcriptional activator design revealed induction ratios of 1.1-fold at 0.1 µM, 2.5-fold at 1 µM, and 3.7-fold at 10 µM pC-HSL (**Supplementary Table 1**). Induction ratios for the SV40 NLS variants were similar (**Supplementary Fig. 1B**), but we selected the BP NLS design for subsequent work because it displayed lower variability across biological replicates. These results indicate that both operator multiplicity and nuclear import affect transcriptional response in plant synthetic circuits.

We next adapted the optimized circuit configuration to enable fluorescence output for studying spatial response patterns in plant tissues. To this end, we replaced GeNL with a nuclear-localized 2×GFP and replaced NanoLuc with a constitutively expressed membrane-localized tdTomato. We also incorporated seed coat marker FAST-Red and BASTA antibiotic resistance cassettes for subsequent use of this construct to generate transgenic lines (**Fig. 1C**)[23].

Transient *N. benthamiana* leaf assay of the optimized GFP circuit via confocal microscopy confirmed strong nuclear-localized fluorescence in response to 0.1 and 1 µM pC-HSL, while untreated leaves displayed minimal signal (**Fig. 1D**). **Supplementary Fig. 2** provides confocal microscopy images from 3 additional biological replicates containing individual plants. Quantification of confocal images across all 4 biological replicates showed a robust, dose-dependent response detectable at as low as 0.1 µM pC-HSL (**Fig. 1E**). The circuit exhibited an 8.2-fold increase at 0.1 µM and a 36-fold increase at 1 µM relative to the untreated control (**Fig. 1E**; **Supplementary Table 2**). These results are consistent with the plate reader-based luciferase assay, with the larger fold changes reflecting the higher sensitivity of fluorescence-based imaging readouts.

### *Stable Arabidopsis lines detect pC-HSL at nanomolar concentrations in roots*

We next generated stably transformed *A. thaliana* lines carrying the optimized pC-HSL-inducible GFP circuit (**Fig. 1C**) to evaluate root responses to exogenous pC-HSL *in vivo*. We treated the seedlings with pC-HSL and imaged the roots using confocal microscopy to analyze activation of the inducible circuit (**Supplementary Fig. 3A**). We generated and screened three independent transgenic lines for reporter responsiveness to pC-HSL. We selected the best-performing line (Line #1) for further characterization (**Supplementary Fig. 4-6**).

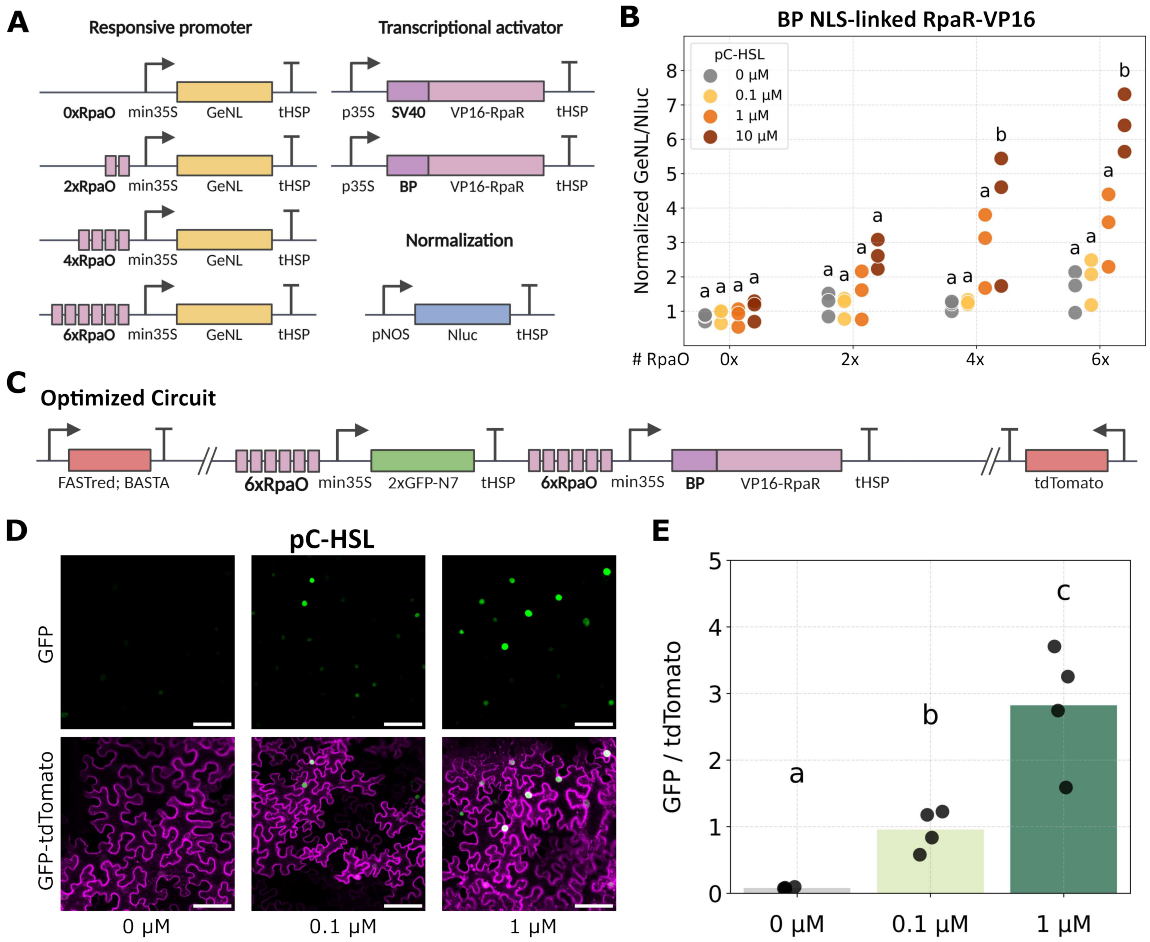



**Figure 1. Optimization of pC-HSL-inducible circuit in *N. benthamiana* transient assays. A)** Schematic of circuit variants combining different RpaO operator site numbers (0x, 2x, 4x, 6x) with alternative nuclear localization signals (SV40 / bipartite BP) driving the RpaR-VP16 transcriptional activator. **B)** GeNL/NanoLuc activity of circuit variants treated with 0, 0.1, 1, 10 µM pC-HSL. N = 3 independent plants. Untreated plants (0 µM) served as controls. **C)** The optimized pC-HSL-inducible circuit contains 6×RpaO-mini35S-2×GFP-N7-tHSP inducible output module, pUBQ10-BP-VP16-RpaR-tHSP transcriptional activator, pUBQ10-tdTomato-tOCS normalization module, and FAST-Red and BASTA selection markers. **D)** Representative confocal microscopy images of n = 4 independent plants for GFP (green) and GFP-tdTomato (magenta) overlay expressing the optimized pC-HSL-inducible circuit treated with 0, 0.1, or 1 µM pC-HSL. Scale bars, 100 µm. **E)** Sensor response quantification as GFP normalized to tdTomato. Bars represent mean ± S.E.M. of 4 independent plants. In panels **B** and **E**, log-transformed data were analyzed by one-way ANOVA with Tukey's HSD post hoc test. Different letters indicate statistically significant differences ($p < 0.05$).

GFP was detected in all roots in response to pC-HSL, while untreated controls exhibited little to no signal (**Fig. 2A**). Quantitative analysis of confocal images across nine biological replicates, collected in two independent experiments, showed that the circuit remained fully functional in root tissues, displaying a detection limit of 0.03 µM pC-HSL and a gradual fluorescence intensity increase up to 1 µM pC-HSL (**Fig. 2B**). Induction at 30 nM pC-HSL was 25-fold compared to the untreated control. Induction in stable lines was substantially higher than in transient *N. benthamiana* assays. Transient expression produced 8.2-fold and 36-fold increases at 0.1 and 1 µM pC-HSL, respectively, whereas stable line #1 achieved 61-fold and 2,600-fold increases at the same concentrations relative to the untreated control (**Supplementary Table 3**).

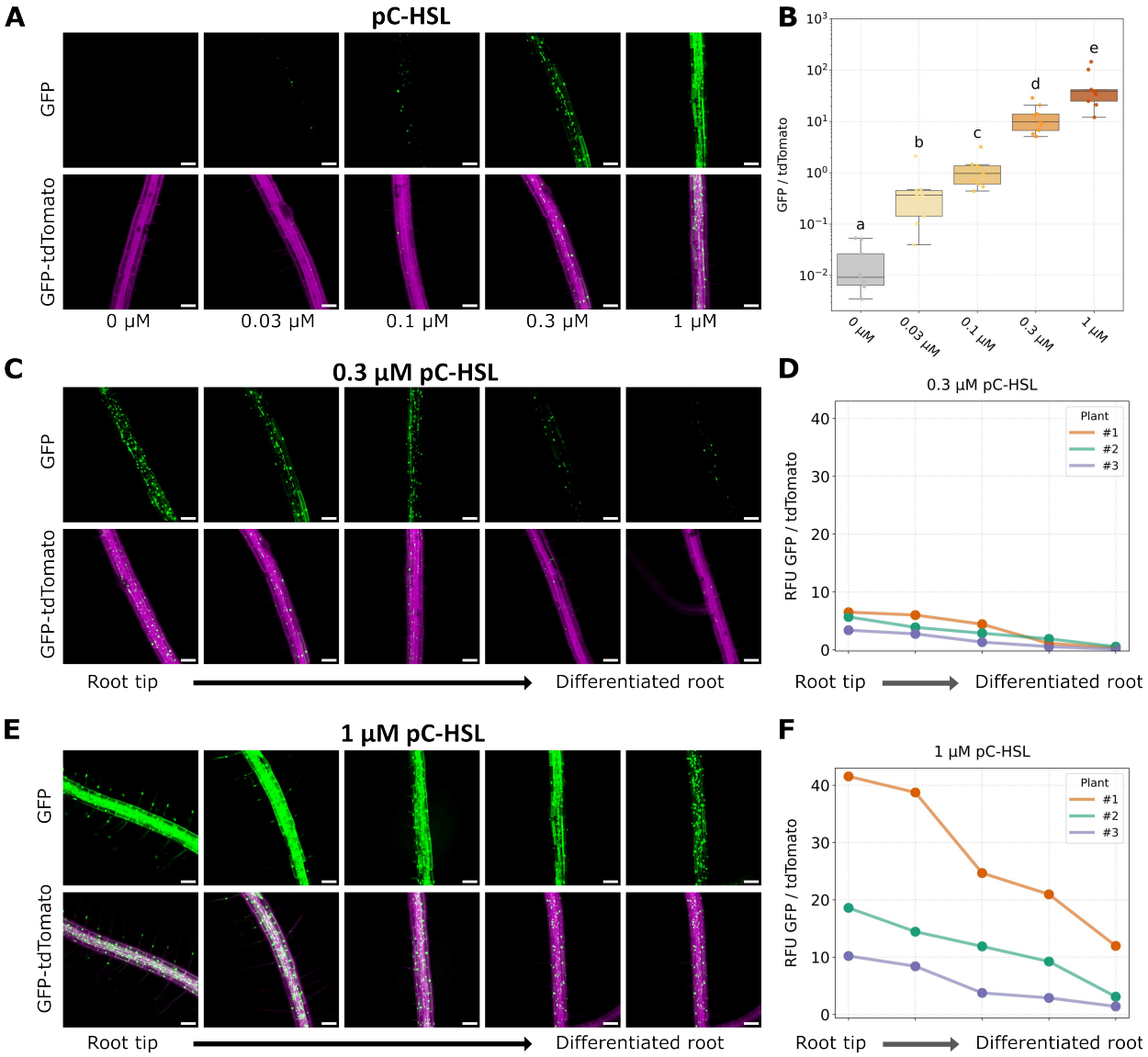



**Figure 2. Stably transformed *A. thaliana* detects pC-HSL at nanomolar concentrations with spatial patterning along the root axis. A)** Representative confocal microscopy images of n = 9 independent plants for GFP (green) and tdTomato (magenta) signals in *A. thaliana* roots treated with pC-HSL at concentrations ranging from 0 to 1 µM. **B)** Quantification of circuit activation in roots of stably transformed *A. thaliana* seedlings from confocal images. GFP fluorescence was measured and normalized to tdTomato in the primary root. Data are shown as boxplots (median, Interquartile Range IQR, and 1.5×IQR whiskers) with individual data points overlaid (n = 9 independent plants). Untreated plants (0 µM) served as controls. Log-transformed data were analyzed by one-way ANOVA with Tukey's HSD post hoc test. Different letters indicate statistically significant differences ($p < 0.05$). **C, E)** Representative images of n = 3 independent plants for the spatial profile of GFP activation along the primary root treated with 0.3 µM and 1 µM pC-HSL. Images are shown from left to right as fields of view progressing from the root tip toward the maturation zone. **D, F)** Quantification of circuit activation along the primary roots when treated with 0.3 µM and 1 µM pC-HSL. Each line represents an independent plant (n = 3). All scale bars, 100 µm.

Notably, the GFP reporter activation was not spatially uniform along the sentinel plant root longitudinal axis. GFP fluorescence was strongest in the root tip and decreased toward the root elongation and maturation regions, as observed in representative confocal microscopy images following treatment with 1 µM or 0.3 µM pC-HSL (**Fig. 2C-D; Supplementary Fig. 7**). Quantification of reporter activation from the confocal microscopy images along the length of individual primary roots across three independent biological replicates confirmed the gradient of GFP response to pC-HSL decreasing from root tip to maturation/differentiation zone (**Fig. 2E, F**).

In addition to the longitudinal GFP analysis, we analyzed the radial response pattern of sentinel roots to pC-HSL treatment. A reconstructed transverse section showed reporter activation across all root cell layers at the highest dose level, 1 µM. GFP fluorescence was most strongly and frequently detected in epidermal and cortical layers and extended toward the endodermis and stele. At lower pC-HSL concentrations of 0.3 µM, little to no activation was observed in the inner endodermis and stele layers, whereas at higher pC-HSL concentrations of 1 µM, reporter activation was frequently detected in all root cell layers (**Supplementary Fig. 8**).

***Root-applied pC-HSL activates reporter expression in sentinel plant leaves***

Having established a sensitive response to pC-HSL in sentinel plant roots, we next investigated whether pC-HSL can travel acropetally to induce a response in leaf tissue, a key property for plants capable of visibly reporting underground rhizosphere activity. We grew sentinel *A. thaliana* lines harboring the optimized circuit on split MS agar plates, in which we applied pC-HSL exclusively to the lower half containing the root system, and we measured the response in leaves after 72 h (**Supplementary Fig. 3B**).

Confocal microscopy revealed fluorescence in leaf tissues at concentrations as low as 1 µM pC-HSL applied to roots, with significantly stronger GFP signal at 3 and 10 µM (**Fig. 3A**). Quantitative analysis of confocal microscopy images across nine biological replicates, collected in two independent experiments, showed that the GFP intensity increased with the concentration of pC-HSL applied to the roots (**Fig. 3B**). For each leaf sample, we captured three fields of view (FOVs) and averaged the integrated fluorescence densities from the entire FOVs to obtain representative measurements (**Supplementary Fig. 9**). The circuit in the leaf exhibited a 2.1-fold increase at 1 µM, a 270-fold increase at 3 µM, and an 840-fold increase at 10 µM relative to the untreated control (**Supplementary Table 4**). This steep increase between 1 and 3 µM pC-HSL suggests a threshold concentration for efficient root-to-shoot relay.

Whole-leaf confocal microscopy imaging of root-treated plants revealed the spatial pattern of sensor response in leaves, showing that the reporter fluorescence was concentrated and stronger in leaf areas near the petiole (**Fig. 3C**). Consistent with this spatial pattern, GFP fluorescence within individual leaves was predominantly localized to areas close to vasculature and veins, with a stronger signal observed in vascular-associated regions (FOV1) compared to non-vascular regions (FOV2 and FOV3) when lower pC-HSL concentrations of 1 and 3 µM were used. At a high pC-HSL concentration of 10 µM, the sensor response was readily detected across all parts of the leaf (**Supplementary Fig. 9**).

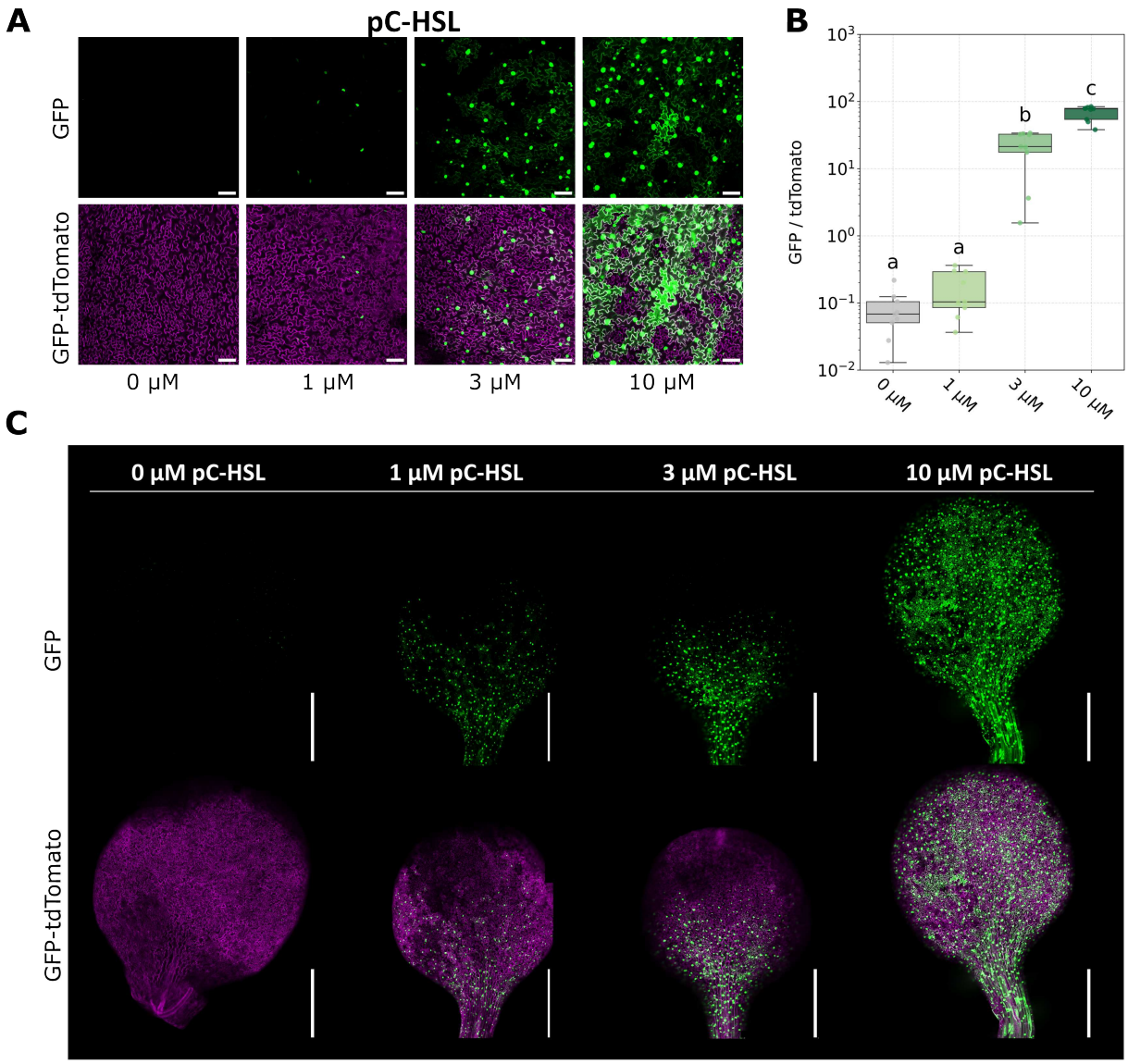



**Figure 3. Root-applied pC-HSL induces dose-dependent reporter activation in sentinel plant leaves.** **A)** Representative confocal images of n = 9 independent plants for GFP (green) and tdTomato (magenta) signals in *A. thaliana* leaves with root-treated pC-HSL at concentrations ranging from 0 to 10 µM. Scale bars, 100 µm. **B)** Quantification of circuit activation in leaves of stably transformed *A. thaliana* seedlings. Data are shown as boxplots (median, Interquartile Range IQR, and 1.5×IQR whiskers) with individual data points overlaid (n = 9 independent plants). Untreated plants (0 µM) served as controls. Log-transformed data were analyzed by one-way ANOVA with Tukey's HSD post hoc test. Different letters indicate statistically significant differences ($p < 0.05$). **C)** Whole-leaf confocal scan of systemic activation. GFP fluorescence is spatially patterned, appearing strongest near the basal areas of the leaf. Top row, GFP; bottom row, GFP (green) and tdTomato (magenta) overlay. Scale bars, 1 mm.

***Sentinel plants detect bacterially produced pC-HSL in root-microbe co-culture systems***

The rhizosphere is a chemically dynamic environment where microbial communities continuously exchange signals with each other and the surrounding plants[24]. To move beyond exogenous chemical induction and toward a system that can directly report native microbial activity, we tested whether pC-HSL produced by engineered bacteria could activate the sentinel plant response. Establishing this capability would allow microbial activity to be encoded as a chemical signal that the sentinel plant detects and reports.

To this end, we reconstructed the pC-HSL biosynthetic pathway in *Escherichia coli* and *Pseudomonas putida*. The synthetic biosynthetic pathway consisted of three enzymes: TAL from *Rhodobacter sphaeroides*, 4CL from *Nicotiana tabacum*, and the pC-HSL synthase RpaI from *Rhodopseudomonas palustris*, which convert L-tyrosine into p-coumarate, p-coumaroyl-CoA, and ultimately pC-HSL, respectively (**Supplementary Fig. 10A**)[18]. The synthetic operon expressed these enzymes with a constitutive promoter and a strong intrinsic terminator (**Supplementary Fig. 10B**). Both engineered strains produced minimal pC-HSL without the precursor and accumulated substantially higher levels when supplemented with p-coumarate, as measured by a fluorescence bioassay (**see Methods**). At 48 h, *E. coli* produced 32.8 µM pC-HSL in the bacterial supernatant when cultured with the precursor p-coumarate and 3.0 µM without, while *P. putida* produced 13.9 µM and 2.1 µM with and without p-coumarate, respectively (**Supplementary Fig. 10C-D**).

We next evaluated whether microbially generated pC-HSL could trigger a detectable response *in planta* using a root-microbe co-culture assay. We grew sentinel *A. thaliana* seedlings on MS agar plates containing p-coumarate and applied bacterial suspensions exclusively to the lower half of the plate to ensure contact only with the root system. After three days of co-cultivation, we measured GFP fluorescence in leaves (**Supplementary Fig. 3C**). Representative confocal images of leaf tissues showed that both engineered *E. coli* and *P. putida* induced strong reporter activation in leaves when roots were inoculated with as low as OD 1 bacteria, with higher bacterial OD leading to progressively stronger GFP signal (**Fig. 4A and C**). Quantitative analysis of confocal microscopy images across six biological replicates showed that, relative to uninoculated controls, *E. coli* induced 15-, 44-, and 140-fold increases in reporter signal at OD 1, 3, and 10, respectively. Similarly, *P. putida* induced 12-, 46-, and 200-fold increases in reporter signal at OD 1, 3, and 10, respectively (**Fig. 4B and D; Supplementary Table 5**).

Because the reporter response at OD 1 (15-fold for *E. coli* and 12-fold for *P. putida*) exceeded that of a 1 µM root-applied pC-HSL standard (2.1-fold) (**Supplementary Tables 4 and 5**), we asked whether lower bacterial densities would still produce detectable activation with longer co-culture periods. We performed a time-course assay spanning three orders of magnitude of bacterial density (OD 0.01, 0.1, and 1) and quantified GFP activation after 3, 5, and 7 days. Beginning at Day 3, only the high-density inoculum (OD 1) elicited a statistically significant response, while low-density inocula remained near baseline for both *E. coli* and *P. putida*. By Days 5 and 7, the OD 1 inoculum reached maximal activation, and lower-density inocula elicited elevated signal activation with both *E. coli* and *P. putida*, particularly at OD 0.1, demonstrating that prolonged co-culture of microbes with plant roots enables robust detection even at low, soil-relevant microbial densities (**Fig. 4E and F**).

Overall, these experiments demonstrate that sentinel plants can detect and report microbially generated pC-HSL from two diverse bacterial species, establishing a functional chemical communication bridge between microbes and plants.

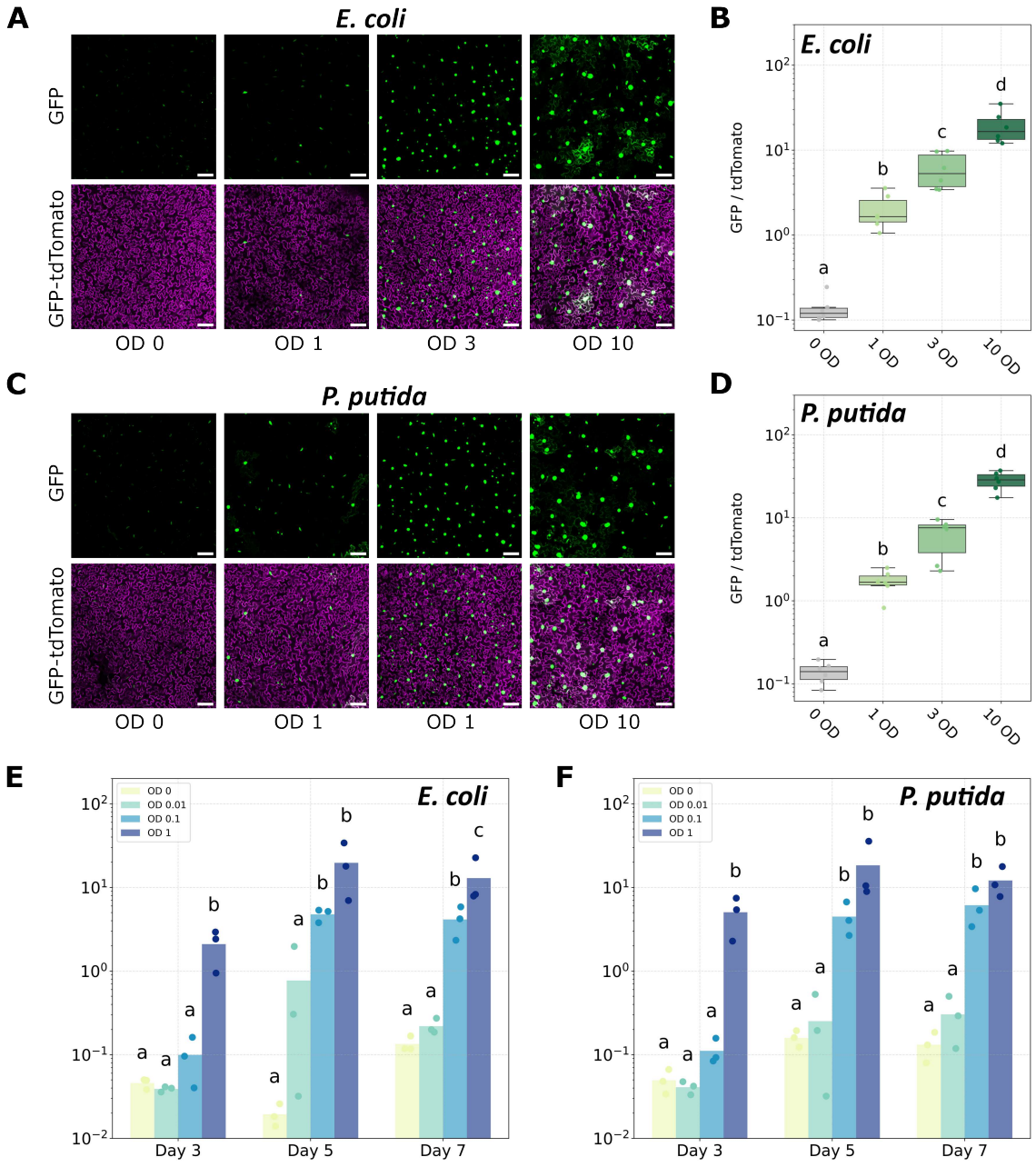



**Figure 4. Sentinel plants detect bacterially secreted pC-HSL in co-culture. A, C)** Representative confocal images of n = 6 independent plants for GFP (green) and tdTomato (magenta) signals in *A. thaliana* leaves with root-treated *E. coli* (top) or *P. putida* (bottom) suspension at OD600 ranging from 0 to 10. Scale bars, 100 µm. **B, D)** Quantification of circuit activation in *A. thaliana* leaves with root-treated *E. coli* (top) or *P. putida* (bottom) suspension. Data are shown as boxplots (median, Interquartile Range IQR, and 1.5×IQR whiskers) with individual data points overlaid (n = 6 independent plants). Uninoculated plants (OD 0) served as controls. Log-transformed data were analyzed by one-way ANOVA with Tukey's HSD post hoc test. Different letters indicate statistically significant differences ($p < 0.05$). **E, F)** Quantification of circuit activation in *A. thaliana* leaves with root-treated *E. coli* (left) or *P. putida* (right) at lower bacterial densities and extended incubation times (3, 5, and 7 days). Bars represent the mean of 3 independent plants. Log-transformed data were analyzed by one-way ANOVA with Tukey's HSD post hoc test. Different letters indicate statistically significant differences ($p < 0.05$).

***Sentinel plants can detect bacterially produced pC-HSL in agricultural soil***

We assessed sentinel plant performance in an agricultural soil to determine whether the platform remains functional in field-relevant conditions. We first performed a dose-response assay in agricultural soil that was mixed with sand to improve aeration and supplemented with 0 to 100 µM pC-HSL. Confocal imaging showed that the sensor response was clearly detectable in leaf tissues at 3 µM pC-HSL and increased progressively at 10, 30, and 100 µM pC-HSL (**Supplementary Fig. 11A**). Quantification across six independent plant replicates revealed that the GFP intensity increased with the concentration of pC-HSL applied to the roots (**Supplementary Fig. 11B**). Sentinel plants grown in soil exhibited a 5.8- and 72-fold increase at 3 and 10 µM pC-HSL, respectively, relative to the untreated control (**Supplementary Table 6**).

We next evaluated whether bacterially produced pC-HSL could be detected in soil. We mixed engineered bacteria with agricultural soil and exposed the roots of *A. thaliana* sentinel seedlings to the inoculated soil (**Fig. 5A**). Representative confocal microscopy images of leaf tissues showed detectable GFP fluorescence in plants grown in soil inoculated with OD 0.1, 1, and 10 bacteria for 72 hours (**Fig. 5B, D**). Quantitative analysis of four independent plants showed that, relative to uninoculated controls, *E. coli* induced a 7-, 43-, and 410-fold increase in reporter signal at OD 0.1, 1, and 10, respectively. Similarly, *P. putida* induced a 2-, 36-, and 230-fold increase in reporter signal at OD 0.1, 1, and 10, respectively. (**Fig. 5C-E; Supplementary Table 7**). Notably, reporter activation in soil exceeded that observed in plate co-culture at equivalent inoculation densities. These results demonstrate that sentinel plants retain functionality in agricultural soil.

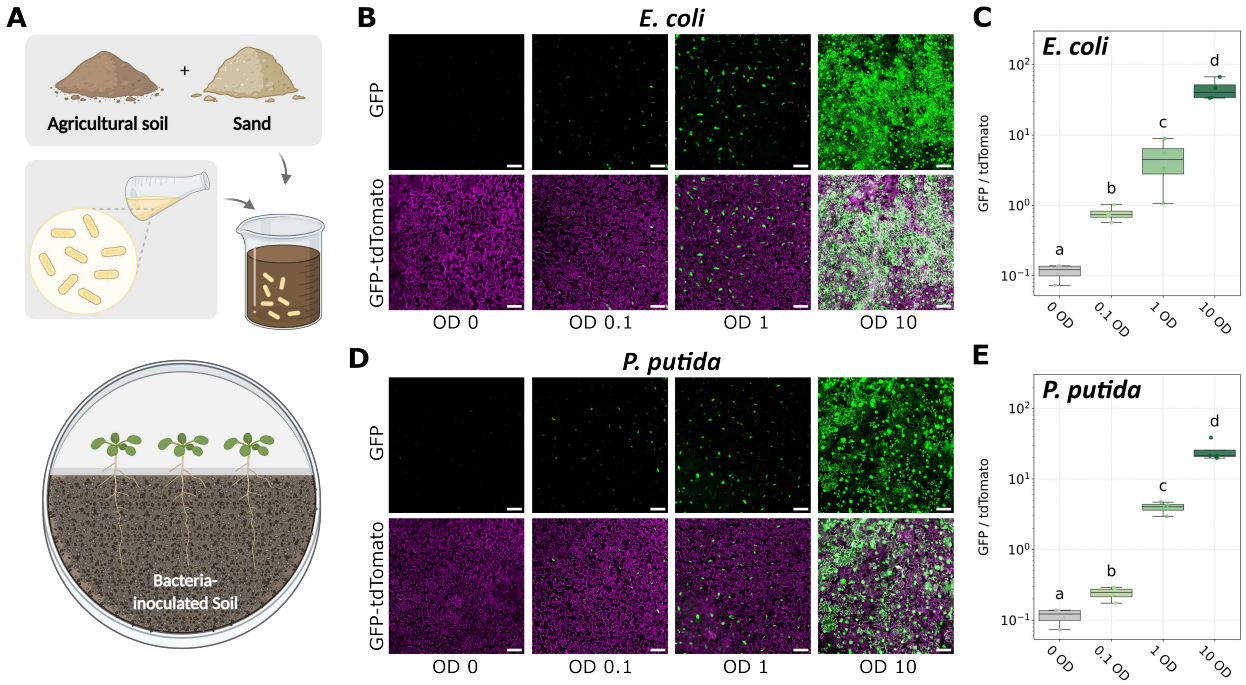



**Figure 5. Sentinel plants detect bacterially secreted pC-HSL in soil. A)** Schematic of the soil assay workflow. Sentinel *A. thaliana* seedlings were grown in split plates where only roots were exposed to bacteria-inoculated soil. **B, D)** Representative confocal images of 6 independent plants for GFP (green) and tdTomato (magenta) signals in *A. thaliana* sentinel plants grown in soil inoculated with engineered *E. coli* (top) or *P. putida* (bottom) suspension at OD600 from 0 to 10. Scale bars, 100 µm. **C, E)** Quantification of circuit activation in *A. thaliana* leaves grown in soil inoculated with engineered *E. coli* (top) or *P. putida* (bottom) grown in soil (n = 4 independent plants). Uninoculated plants (OD 0) served as controls. Data are shown as boxplots (median, interquartile range IQR, and 1.5×IQR whiskers) with individual data points overlaid. Log-transformed data were analyzed by one-way ANOVA with Tukey's HSD post hoc test. Different letters indicate statistically significant differences ($p < 0.05$).

## Discussion

In this study, we established sentinel plants that convert invisible rhizosphere microbial signals into visible, systemic aboveground readouts, demonstrating that plant-encoded circuits can serve as noninvasive monitors of soil microbial activity.

We showed that transient expression screening in *N. benthamiana* using high-throughput, quantitative reporters, such as luciferase, provides a first-pass strategy to optimize circuit architecture, including operator multiplicity and transcription-factor configuration. The transient assays enabled rapid identification of high-performing designs prior to committing to stable transformation. Upon transferring this optimized pC-HSL circuit into *A. thaliana* to generate stable lines, we demonstrated a dynamic range of induction in roots reaching a 2600-fold response upon treatment with 1 μM pC-HSL compared to a 36-fold response observed in transient *N. benthamiana* assays. This enhanced performance likely reflects higher expression of the RpaR-VP16 activator in the transgenic background, resulting in stronger promoter occupancy and transcriptional activation.

Alongside prior demonstrations of the functionality of canonical acyl-HSLs, our results showed that non-canonical quorum-sensing systems are also functional in plants[25]. Synthetic circuits based on quorum-sensing pathways are largely orthogonal to endogenous plant signaling pathways, making them attractive and transferable components for plant sensors across species[26]. Future optimization of sentinel circuits in crop species could leverage rapid transient testing methods, such as VAST[27].

The spatial patterns of pC-HSL-inducible reporter activation in roots indicate that longitudinal developmental gradients and radial diffusion barriers jointly shape signal perception. The endodermis forms a selective diffusion barrier by depositing suberin-rich Casparian strips that block apoplastic transport[28]. Along the longitudinal axis, stronger reporter activation near the root tip compared to more mature regions is consistent with the developmental state of the endodermis. In younger root tissues, incomplete Casparian strip formation and limited suberin deposition reduce diffusion barriers[29,30]. Along the radial axis, reporter activation at lower pC-HSL concentrations was primarily confined to epidermal and cortical layers, which are outer root tissues. In contrast, higher concentrations enabled activation in the endodermis and stele, indicating that the Casparian strip may limit signal penetration in a concentration-dependent manner. Future work can test these hypotheses using *Arabidopsis* barrier mutants.

Previous work in *Hordeum vulgare* has shown that inhibition of ATP-dependent ABC transporters by orthovanadate reduces uptake of canonical acyl-HSLs, while KCl-induced plasmodesmatal closure impairs long-distance symplastic transport, indicating that HSL movement in roots involves both active uptake and symplastic transport[25]. Further investigation will be required to determine whether similar pathways mediate pC-HSL transport in plant tissues and from root to shoots. Pharmacological inhibition assays and radiolabeled pC-HSL tracking could directly address this question.

Beyond localized sensing within the roots, our results demonstrate that pC-HSL applied exclusively to roots can be transported systemically through the vasculature, reaching leaves via the stem and major veins. In Boo et al., reporter fluorescence remained undetectable in leaves. This difference may reflect improved circuit sensitivity in our system, enabled by increased RpaO copy number, strong nuclear localization of RpaR, and nuclear-localized reporter accumulation[16]. We observed that reporter activation was spatially heterogeneous, both among different leaves and within individual leaves. GFP fluorescence was stronger in mature leaves than in newly developing leaves and was localized in leaf parts closer to the petiole and veins. This developmental pattern likely reflects reduced accumulation of the RpaR-VP16 transcriptional activator in developing leaves, and consequently, mature leaves exhibited greater signal-

activation capacity than juvenile tissues. The spatial confinement of reporter activation closer to the petiole and veins suggests that signal molecule availability in distal leaf regions may be limited.

These observations highlight an important design principle for plant-based biosensor design. Our findings indicate that sensor performance is not solely dictated by circuit architecture or signal concentration, but also by tissue developmental state and spatial competence for signal decoding. To engineer more versatile plant sensors, signal perception may be gated at the tissue or cell-type level. Such gating can involve two distinct factors: whether a signaling molecule can reach a given cell, and whether that cell can activate a transcriptional response. The former is governed by plant physiology and tissue architecture, and the latter can be genetically programmed, for example, using cell-type-specific promoters to control transcriptional regulators or essential components of the output module in target organs[31,32]. Such strategies will be essential for extending plant-based biosensing platforms to more mature plants and field-relevant conditions, where tissue heterogeneity and developmental complexity are unavoidable.

The availability of the precursor p-coumarate is a determinant of pC-HSL production by the engineered bacteria[33]. In soil environments, this requirement may be readily met, as p-coumarate is a phenylpropanoid derived from plant lignin and has been detected in root exudates and rhizosphere soils, where it can accumulate to levels exceeding 20 mg/kg[34,35]. Thus, plants themselves may serve as a natural source of precursor molecules. More broadly, precursor-dependent signaling systems could be leveraged to couple bacterial activity to plant presence. This strategy could be extended to enable controllable bacterial behaviors, including root-associated activation and biocontainment mechanisms, for example, by placing pC-HSL biosynthesis under the control of plant-derived precursors to restrict signaling to the rhizosphere.

Another consideration is the microbial density required to detect a signal. In our co-culture assays, detectable leaf-level responses were observed at an inoculation density of OD 0.1, corresponding to approximately $0.8 \times 10^8$ cells $mL^{-1}$. Given that bacterial abundances in the rhizosphere can reach up to ~$10^{11}$ microbial cells per gram of root, and bulk soil typically has lower densities of $10^8$-$10^9$ cells per gram[36], this observation highlights opportunities for future optimization, including enhancement of microbial signal biosynthesis, improved root colonization, and incorporation of signal amplification or relay architectures within the plant circuit to improve detection thresholds.

Lastly, we demonstrated the sentinel plant's functionality in agricultural soil, showing responsiveness to both exogenously applied and bacterially produced pC-HSL. At OD 1 inoculation densities, reporter activation fold change in soil (43 for *E. coli* and 36 for *P. putida*) was greater than that observed in plate assays (15 for *E. coli* and 12 for *P. putida*). Despite the increased biotic and abiotic complexity of the unsterile agricultural soil matrix, engineered bacteria grew and produced pC-HSL, and the signaling molecule remained sufficiently mobile to activate the reporter circuit in the leaves of sentinel plants. Nonetheless, additional mesoscale chambers and controlled greenhouse trials will be necessary to evaluate reproducibility, stability, robustness, and long-term performance before advancing the sentinel plant platform toward field deployment.

Our findings outline the core components of a sensitive biosensing platform that reports microbial processes through a plant-encoded aboveground signal. Although this study utilized constitutive production of the signaling molecule, the bacterial module can be readily reprogrammed for inducible operation, linking sensor output to endogenous bacterial transcriptional states or to promoters responsive to specific rhizosphere cues[37,38]. By providing continuous, non-destructive, and scalable access to key microbial dynamics, this sentinel plant platform can advance long-term soil management, precision agriculture, and ecosystem monitoring.

## Methods

### *Construct design and cloning*

The core pC-HSL-inducible cassette was kindly provided by the Christopher Voigt lab[16]. Plasmids were assembled with the Loop Assembly method using BsaI- and SapI-mediated Golden Gate reactions (NEB catalog numbers R0569S and E1601L, respectively) and cloned into pCAMBIA backbones. All plasmids were propagated in NEB Turbo *Escherichia coli* competent cells (NEB catalog no. C2984I) and sequence-verified by nanopore sequencing (Plasmidsaurus). Plasmids generated in this work are listed in **Supplementary Table 8**.

### *Plant growth conditions*

*A. thaliana* (Col-0) seeds were surface-sterilized by exposure to chlorine gas. Chlorine gas was produced by mixing 100 mL of bleach with 3 mL of 6 N hydrochloric acid. The mixture was placed in a desiccator box within a chemical fume hood, and the seeds were exposed to chlorine gas for at least 3 hours. Seeds were germinated on ½ MS plates containing 0.5x Murashige and Skoog Basal Salt Mixture (M524, PhytoTech Labs), 0.05% MES (w/v), 0.7% Phytagel (P8169, Millipore Sigma), pH 5.7, and incubated in a growth chamber at 22°C with a 16/8 h light/dark cycle. *Nicotiana benthamiana* plants were grown in controlled growth chambers (Conviron) under long-day conditions (16 h light / 8 h dark) set to 22°C.

### *N. benthamiana transient luciferase assay*

*Agrobacterium tumefaciens* GV3101 strains harboring circuit constructs were cultured overnight at 30 °C with shaking at 200 rpm in 2×YT medium (ThermoFisher 22712020) supplemented with 10 μg $mL^{-1}$ rifampicin (Sigma-Aldrich R3501), 20 μg $mL^{-1}$ gentamicin (Sigma-Aldrich G1264), 50 μg $mL^{-1}$ tetracycline (Sigma-Aldrich T7660), and 50 μg $mL^{-1}$ kanamycin (Sigma-Aldrich K1637). Cultures were pelleted by centrifugation at 4,000 g for 5 min and resuspended in infiltration buffer (10 mM MES, pH 5.7; 10 mM $MgCl_2$; 200 μM acetosyringone) to a final $OD_{600}$ of 0.4. Resuspended cultures were incubated at room temperature with shaking at 120 rpm for 4 h to induce virulence gene expression prior to infiltration.

Agrobacterium suspensions were infiltrated into the abaxial surface of fully expanded leaves of 3-4-week-old *N. benthamiana* plants using a needleless syringe. At 48 h post-infiltration, the same leaf areas were infiltrated with pC-HSL (Millipore Sigma 07077-50MG) at concentrations ranging from 0 to 10 μM. Leaf tissue was harvested 48 h after pC-HSL treatment for luciferase analysis.

For luminescence measurements, three leaf discs were excised from infiltrated leaf areas using a 1/4″ radius leaf punch and placed into 2 mL microcentrifuge tubes (Fisher Scientific 15-340-162) containing 2.8 mm ceramic beads (Fisher Scientific 15-340-160). Samples were immediately flash-frozen in liquid nitrogen and homogenized using a mini bead-beater tissue homogenizer (Fisher Scientific 15-340-164) for two 20-s cycles at maximum speed. Following homogenization, 200 μL of 1× Cell Lysis Buffer (Promega E1531) was added to each tube, and samples were vortexed vigorously until fully resuspended. Lysates were incubated on ice for 10 min and clarified by centrifugation at 12,000 g for 5 min to pellet cellular debris.

Luciferase activity was measured using the Nano-Glo® Luciferase Assay System (Promega N1110) according to the manufacturer's instructions with minor modifications. Briefly, 30 μL of clarified lysate was mixed with 60 μL of Nano-Glo reagent in a 96-well plate (Fisher Scientific 07-200-627). Luminescence was recorded using a Tecan Spark plate reader at 25°C with a 1 s integration time per well. GeNL and NanoLuc signals were collected using 520–590 nm and 430–485 nm emission filters, respectively. Signal deconvolution coefficients were calculated by measuring total, GeNL-only, and NanoLuc-only luminescence and applying the Promega ChromaLuc Technology calculator (Technical Manual TM062).

***A. thaliana floral spray transformation and selection***

*Agrobacterium tumefaciens* cultures (50 mL) harboring the appropriate plant expression constructs were grown to the stationary phase, pelleted by centrifugation at 4,000 g for 10 min, and resuspended in 5% (w/v) sucrose supplemented with 0.02% (v/v) Silwet L-77 (Fisher Scientific NC1765106). Flowering *A. thaliana* plants (6-7 weeks old) were uniformly sprayed with the *Agrobacterium* suspension until runoff[39]. Plants were covered overnight with a light-blocking dome to maintain humidity and minimize light exposure, then returned to standard growth conditions.

Upon seed maturation, T1 seeds were screened for FAST-Red fluorescence, and positive seeds were picked out and germinated on ½ MS agar plates supplemented with 5 μg $mL^{-1}$ glufosinate ammonium (BASTA; Millipore Sigma 45520-100MG) to select for resistant transformants. Multiple independent lines were screened for reporter responsiveness, and a single high-performing homozygous line was selected for downstream experiments.

***Confocal microscopy and fluorescence quantification***

Plant samples were mounted in distilled water and imaged immediately using a Leica Stellaris 8 confocal laser-scanning microscope equipped with an HC PL APO 10×/0.40 CS2 objective, housed in the Biological Imaging Facility (BIF) at Caltech. A pulsed white-light laser at 488 nm was used to excite GFP, and emission spectra were collected between 500 and 540 nm. The pulsed white light laser set to 561 nm was used to excite tdTomato fluorescence, and emission was collected between 580 and 630 nm. For single-frame imaging, one optical z-section was acquired per field of view with the pinhole set to 10 AU. For z-stack acquisition, optical sections were collected sequentially with the pinhole set to 1 AU and a z-step size of 5 μm. Identical laser power, detector gain, and offset settings were maintained for all samples within each experiment. Images were exported from Leica LAS X software (v4.3) as 16-bit TIFF files.

Each data point represents the average across multiple FOVs from a single biological replicate corresponding to a single plant. 6 to 9 biological replicates were used in these experiments (see Figure captions). For *N. benthamiana* leaves, a leaf punch adjacent to the infiltration site was collected. The mean fluorescence intensity of each biological replicate was calculated from 4 random non-overlapping FOVs within the same punch. For *A. thaliana* leaves, the mean fluorescence intensity of each biological replicate was calculated from 3 random non-overlapping FOVs of the same leaf. For *A. thaliana* roots, each datapoint corresponds to a single FOV. The fluorescence intensity of each FOV was calculated in Fiji/ImageJ using the “integrated density” option, which measures the sum of pixel intensity values within a selected region of interest, with the region set to the entire FOV. Fold-change was calculated as the ratio of integrated GFP to tdTomato fluorescence intensity, multiplied by 100.

***Chemical induction of sentinel plant roots with pC-HSL***

Transgenic *A. thaliana* seedlings were grown vertically on ½ MS agar plates for 10 days. Seedlings were then transferred to ½ MS agar plates supplemented with defined concentrations of pC-HSL. Plates were maintained in a vertical orientation to preserve root architecture. After 48 h of induction, seedling roots were imaged by confocal microscopy as described.

***Chemical induction of sentinel plant leaves with pC-HSL***

Transgenic *A. thaliana* seedlings were grown vertically on ½ MS agar plates for 10 days. Seedlings were then transferred to vertically oriented split agar plates (I-plates; VWRU25384-344). The lower compartment of the petri dish contained ½ MS agar supplemented with defined concentrations of pC-HSL, while the upper compartment contained ½ MS agar without any inducer. Roots were positioned in the lower compartment, and shoots were exclusively placed in the upper compartment, ensuring that leaves did not contact pC-HSL-containing media. Plates

were maintained in a horizontal orientation. After 72 h of induction, seedling leaves were imaged by confocal microscopy.

***Construction of pC-HSL-producing E. coli and Pseudomonas putida strains***

To construct the pC-HSL production cassette, the three-gene pC-HSL production operon from Du et al.[19] was commercially synthesized as a dsDNA fragment with BsaI overhangs, following the standard CIDAR MoClo Assembly format[40]. This operon was then combined with the J23101 constitutive promoter and a transcriptional terminator and cloned into a kanamycin-resistant p15a vector using 3G assembly[41]. The resulting plasmid was then transformed into chemically competent *E. coli* JM109 cells by adding 1 µL of plasmid assembly product to 50 µL of competent cells and incubating on ice for 10 minutes, after which a 42°C heat shock was applied for 1 minute. After 3 minutes of additional ice incubation, 1 mL of SOC media was added to the cells, and they were grown for 1 hour at 37°C with shaking at 250 rpm, then plated on LB agar plates with 50 µg $mL^{-1}$ kanamycin selection. Colonies from these plates were then grown up and miniprepped to isolate the plasmid, which was validated using whole-plasmid sequencing.

The *E. coli* pC-HSL production strain was constructed by transforming the resulting plasmid into chemically competent *E. coli* BW25113 cells using the heat shock protocol described above. Similarly, the *P. putida* pC-HSL production strain was constructed as follows. Electrocompetent *Pseudomonas putida* KT2440 cells were thawed on ice immediately prior to transformation. Purified plasmid DNA (100-500 ng) was added to 40 µL of competent cells, and the mixture was gently mixed. The cell and plasmid mixture was transferred to a pre-chilled 0.1 cm gap electroporation cuvette (Bio-Rad 652089) and incubated on ice for 10 min. Electroporation was performed using a Bio-Rad MicroPulser electroporator at 2.5 kV. Immediately following the pulse, 500 µL of SOC medium was added to the cuvette, and the cells were transferred to a 1.5 mL microcentrifuge tube. Cells were recovered by incubation at 30°C with shaking at 200 rpm for 2 h, then plated on selective agar and incubated overnight at 30°C.

***Construction of pC-HSL-responsive E. coli biosensor***

We constructed a pC-HSL-responsive GFP biosensor by using 3G Assembly on parts sourced from the CIDAR MoClo Part Extension Kit Volume 1[42]. Notably, the specific sequences of the pC-HSL-responsive transcription factor RpaR and its cognate promoter $P_{rpa}$ were from previously reported engineered variants[43]. The resulting plasmid assembly was transformed into *E. coli* JM109 cells and validated as described above. These strains were used directly as the pC-HSL biosensor.

***Measurement of pC-HSL production from engineered E. coli and P. putida***

The *E. coli* pC-HSL sensor strain was grown overnight in M9CA medium (Teknova M8010) at 30°C with shaking at 200 rpm. On the day of the bioassay, the overnight culture was diluted 1:100 into 5 mL of M9CA medium and incubated for 3 h at 30°C, shaking at 200 rpm to reach the exponential phase. This culture was then diluted an additional 1:100, and 200 µL aliquots were dispensed into a 96-well plate (Fisher Scientific FB012931) for downstream assays.

Engineered *E. coli and P. putida* strains were revived from glycerol stocks and grown overnight in M9CA medium at 30°C with shaking at 200 rpm. Cultures were then diluted to a starting $OD_{600}$ of 0.01 in 3 mL of M9CA medium, with or without 100 µM p-coumarate (Millipore Sigma C9008), in a 24-deep-well plate (ThermoFisher Scientific 95040470). Cultures were incubated at 30°C with shaking at 200 rpm, and 100 µL samples were collected from the same well every 12 h. Samples were centrifuged to pellet bacteria, and the clarified supernatants were retained at -20°C for later analysis.

On the day before the bioassay to measure pC-HSL concentrations in these samples, the *E. coli* pC-HSL sensor strain was revived from glycerol stocks and grown overnight in M9CA medium at

30°C with shaking at 200 rpm. This overnight culture was then diluted 1:100 into 5 mL of M9CA medium and incubated for 3 h at 30°C and 200 rpm to reach the exponential growth phase. This culture was then diluted an additional 1:100 into 200 µL aliquots in a 96-well plate (Fisher Scientific FB012931).

Purified pC-HSL (Sigma-Aldrich 07077) was used to generate a 12-point standard curve spanning 1 nM to 100 µM pC-HSL, which was applied to three technical replicates of the *E. coli* biosensor to calibrate its response to known concentrations of pC-HSL. For each plate, 2 µL of each collected supernatant sample was added to the prepared sensor strain solution. sfGFP fluorescence was measured every 20 min for 24 h of incubation at 30°C with shaking using a Tecan Spark plate reader. Fluorescence values from the supernatants of the production strains were compared against the calibration curve via linear regression to calculate the observed pC-HSL in the sample wells, which is 1/100 of the concentration in the original supernatant. In cases where fluorescence values from the supernatants fell outside the linear range of the biosensor response, the experiments were repeated, with the supernatant samples further diluted as needed to bring the biosensor response within the linear range of the calibration curve.

***Plant-microbe co-culture assay***

Engineered bacterial strains were grown overnight in 5 mL M9CA medium supplemented with p-coumarate at 30°C with shaking. The following day, 200 µL of the overnight culture was inoculated into 20 mL of fresh M9CA medium supplemented with 100 µM of p-coumarate and grown for an additional 24 h. Bacterial cultures were harvested by centrifugation at 4,000 g for 5 min and resuspended in fresh M9CA medium to the desired optical density.

Transgenic *A. thaliana* seedlings were grown vertically on ½ MS agar plates for 10 days. Seedlings were then transferred to vertically oriented split agar plates. The lower compartment of the petri dish contained ½ MS agar supplemented with 100 µM of p-coumarate. A total volume of 400 µL of the bacterial suspension was applied evenly to the lower compartment. Roots were placed in the lower compartment, and shoots were placed exclusively in the upper compartment, ensuring that leaves did not contact the bacterial solution. Plates were maintained in a horizontal orientation. After 72 h of induction, seedling leaves were imaged by confocal microscopy.

***Soil preparation***

Agricultural soil was collected from a post-harvest field site at the University of California, Riverside Agriculture Experiment Station. Soil was collected, sieved through a 1 mm sieve, and stored at 4°C until the start of the experiment. For plant experiments, the soil mixture consisted of 10% (v/v) agricultural soil and 90% (v/v) sand. Solution was added at 20% (v/w) of the total soil mass to achieve an optimal moisture content for plant growth.

***Chemical induction of sentinel plant leaves with pC-HSL in soil***

Transgenic *A. thaliana* seedlings were grown vertically on ½ MS agar plates for 10 days. Seedlings were then transferred to a split petri dish. The lower compartment of the petri dish contained 20 g of soil supplemented with defined concentrations of pC-HSL, while the upper compartment contained 20 g of soil without any inducer. Roots were positioned in the lower compartment, and shoots were exclusively placed in the upper compartment. Plates were maintained in a horizontal orientation. After 72 h of induction, seedling leaves were imaged by confocal microscopy.

***Plant-microbe co-culture assay in soil***

The co-culture medium consisted of M9CA medium and MS medium mixed at a 1:1 (v/v) ratio and supplemented with 100 µM p-coumarate. Engineered bacterial strains were grown overnight in 10 mL co-culture medium at 30°C with shaking. The following day, 4 mL of the overnight culture

was inoculated into 20 mL of co-culture medium and grown for approximately 6 h to reach the exponential phase. Bacterial cultures were harvested by centrifugation at 4,000 g for 5 min and resuspended in fresh co-culture medium to the desired optical density.

Transgenic *A. thaliana* seedlings were grown vertically on ½ MS agar plates for 10 days. Seedlings were then transferred to a vertically oriented split petri dish. The lower compartment of the petri dish contained 20 g of soil watered with a bacterial solution, while the upper compartment contained 20 g of soil without any bacterial solution. Roots were placed in the lower compartment, and shoots were placed exclusively in the upper compartment, ensuring that leaves did not contact the bacterial solution. Plates were maintained in a horizontal orientation. After 72 h of induction, seedling leaves were imaged by confocal microscopy.

**Data Availability Statement**

All data are included either in the manuscript or supplementary files.

**Conflict of Interest Statement**

Authors declare no conflict of interest.

**Author Contributions**

Conceptualization: YW, JPM, GSD
Methodology: YW, JPM, PT
Data Acquisition: YW, JPM, EL, PT, CB
Supervision: GSD
Writing: YW, GSD
Funding Acquisition: JPM, EM, GSD

**Acknowledgements**

The authors thank the RSI Impact Grant team, Bruce Hay, Niles Pierce, Shuwen (Eric) Lei, and Mikhail Hanewich-Hollatz for valuable discussions and feedback. The authors acknowledge the Caltech Biological Imaging Facility, support from the Caltech Beckman Institute, and the Arnold and Mabel Beckman Foundation for providing access to the Leica STELLARIS 8 inverted confocal microscope. Schematics were created with BioRender.com.

**Funding**

This work was supported by the Caltech startup funds, RSI Impact Grant, FFAR (Foundation for Food & Agriculture Research) Fellows program, Caltech Space-Health Innovation Fund, Henry Luce Foundation, and Shurl and Kay Curci Foundation. The Meyerowitz laboratory is also supported by the Howard Hughes Medical Institute. This article is subject to HHMI's Open Access to Publications policy. HHMI lab heads have previously granted a nonexclusive CC BY 4.0 license to the public and a sublicensable license to HHMI in their research articles. Pursuant to those licenses, the author-accepted manuscript of this article can be made freely available under a CC BY4.0 license immediately upon publication.

## References


1. Ahkami, A. H. *et al.* Emerging sensing, imaging, and computational technologies to scale nano-to macroscale rhizosphere dynamics – Review and research perspectives. *Soil Biology and Biochemistry* **189**, 109253 (2024).
2. Del Valle, I. *et al.* Translating New Synthetic Biology Advances for Biosensing Into the Earth and Environmental Sciences. *Front. Microbiol.* **11**, (2021).
3. Jones, E. M., Marken, J. P. & Silver, P. A. Synthetic microbiology in sustainability applications. *Nat Rev Microbiol* **22**, 345–359 (2024).
4. DeAngelis, K. M., Ji, P., Firestone, M. K. & Lindow, S. E. Two Novel Bacterial Biosensors for Detection of Nitrate Availability in the Rhizosphere. *Applied and Environmental Microbiology* **71**, 8537–8547 (2005).
5. Zeng, N., Wu, Y., Chen, W., Huang, Q. & Cai, P. Whole-Cell Microbial Bioreporter for Soil Contaminants Detection. *Front. Bioeng. Biotechnol.* **9**, (2021).
6. Larsson, E. M., Murray, R. M. & Newman, D. K. Engineering the Soil Bacterium Pseudomonas synxantha 2–79 into a Ratiometric Bioreporter for Phosphorus Limitation. *ACS Synth. Biol.* **13**, 384–393 (2024).
7. Chemla, Y. *et al.* Hyperspectral reporters for long-distance and wide-area detection of gene expression in living bacteria. *Nat Biotechnol* 1–11 (2025) doi:10.1038/s41587-025-02622-y.
8. Pfotenhauer, A. C. & Lenaghan, S. C. Phytosensors: harnessing plants to understand the world around us. *Current Opinion in Biotechnology* **87**, 103134 (2024).
9. Khakhar, A. *et al.* Building customizable auto-luminescent luciferase-based reporters in plants. *eLife* **9**, e52786 (2020).
10. Antunes, M. S. *et al.* Programmable Ligand Detection System in Plants through a Synthetic Signal Transduction Pathway. *PLOS ONE* **6**, e16292 (2011).
11. Park, S.-Y. *et al.* An orthogonalized PYR1-based CID module with reprogrammable ligand-binding specificity. *Nat Chem Biol* **20**, 103–110 (2024).
12. Sears, R. G. *et al.* Engineered gamma radiation phytosensors for environmental monitoring. *Plant Biotechnology Journal* **21**, 1745–1756 (2023).
13. Fethe, M. H. *et al.* The performance of pathogenic bacterial phytosensing transgenic tobacco in the field. *Plant Biotechnology Journal* **12**, 755–764 (2014).
14. Home - InnerPlant - Making living sensors. https://innerplant.com/ (2025).
15. Exactly when. Precisely where. Only if. *Insignum AgTech* https://www.insignumagtech.com.
16. Boo, A. *et al.* Synthetic microbe-to-plant communication channels. *Nat Commun* **15**, 1817 (2024).
17. Schaefer, A. L. *et al.* A new class of homoserine lactone quorum-sensing signals. *Nature* **454**, 595–599 (2008).
18. Kang, S.-Y., Lee, J. K., Jang, J.-H., Hwang, B. Y. & Hong, Y.-S. Production of phenylacetyl-homoserine lactone analogs by artificial biosynthetic pathway in Escherichia coli. *Microbial Cell Factories* **14**, 191 (2015).
19. Du, P. *et al.* De novo design of an intercellular signaling toolbox for multi-channel cell–cell communication and biological computation. *Nat Commun* **11**, 4226 (2020).
20. Muñoz-Díaz, E. & Sáez-Vásquez, J. Nuclear dynamics: Formation of bodies and trafficking in plant nuclei. *Front. Plant Sci.* **13**, (2022).
21. Suzuki, K. *et al.* Five colour variants of bright luminescent protein for real-time multicolour bioimaging. *Nat Commun* **7**, 13718 (2016).
22. Cai, Y.-M. *et al.* Rational design of minimal synthetic promoters for plants. *Nucleic Acids Res* **48**, 11845–11856 (2020).
23. Shimada, T., Ogawa, Y., Shimada, T. & Hara-Nishimura, I. A non-destructive screenable marker, OsFAST, for identifying transgenic rice seeds. *Plant signaling & behavior* **6**, 1454–1456 (2011).

24. Berruto, C. A. & Demirer, G. S. Engineering agricultural soil microbiomes and predicting plant phenotypes. *Trends in Microbiology* **32**, 858–873 (2024).
25. Sieper, T. *et al.* N-acyl-homoserine lactone uptake and systemic transport in barley rest upon active parts of the plant. *New Phytologist* **201**, 545–555 (2014).
26. Palmer, A. G., Senechal, A. C., Mukherjee, A., Ané, J.-M. & Blackwell, H. E. Plant Responses to Bacterial N-Acyl l-Homoserine Lactones are Dependent on Enzymatic Degradation to l-Homoserine. *ACS Chem. Biol.* **9**, 1834–1845 (2014).
27. Li, E. *et al.* Vacuum and Sonication Treatment Enable Efficient Transient Gene Expression in Various Monocot and Eudicot Plant Seedlings. *ACS Synth. Biol.* https://doi.org/10.1021/acssynbio.5c00855 (2026) doi:10.1021/acssynbio.5c00855.
28. Naseer, S. *et al.* Casparian strip diffusion barrier in Arabidopsis is made of a lignin polymer without suberin. *Proceedings of the National Academy of Sciences* **109**, 10101–10106 (2012).
29. Alassimone, J., Naseer, S. & Geldner, N. A developmental framework for endodermal differentiation and polarity. *Proceedings of the National Academy of Sciences* **107**, 5214–5219 (2010).
30. Barberon, M. The endodermis as a checkpoint for nutrients. *New Phytologist* **213**, 1604–1610 (2017).
31. Kozaeva, E. & Brophy, J. A. N. Getting to the root of the pattern. *Science* **390**, 24–25 (2025).
32. Borowsky, A. T. & Bailey-Serres, J. Rewiring gene circuitry for plant improvement. *Nat Genet* **56**, 1574–1582 (2024).
33. Hirakawa, H. *et al.* Activity of the Rhodopseudomonas palustris p-Coumaroyl-Homoserine Lactone-Responsive Transcription Factor RpaR. *J Bacteriol* **193**, 2598–2607 (2011).
34. Zhang, J. *et al.* Rhizosphere Microbiome and Phenolic Acid Exudation of the Healthy and Diseased American Ginseng Were Modulated by the Cropping History. *Plants* **12**, 2993 (2023).
35. Zhang, H. *et al.* Phenolic Acids Released in Maize Rhizosphere During Maize-Soybean Intercropping Inhibit Phytophthora Blight of Soybean. *Front. Plant Sci.* **11**, (2020).
36. Berendsen, R. L., Pieterse, C. M. J. & Bakker, P. A. H. M. The rhizosphere microbiome and plant health. *Trends in Plant Science* **17**, 478–486 (2012).
37. Kozaeva, E. *et al.* Roots of synthetic ecology: microbes that foster plant resilience in the changing climate. *Current Opinion in Biotechnology* **88**, 103172 (2024).
38. Li, E. *et al.* Sentinel plants enable quantitative monitoring of bioavailable nitrate in soils and microbial environments. *bioRxiv* 2026.03.18.712767 (2026) doi:10.64898/2026.03.18.712767.
39. Chung, M.-H., Chen, M.-K. & Pan, S.-M. Floral Spray Transformation Can Efficiently Generate Arabidopsis. *Transgenic Res* **9**, 471–486 (2000).
40. Iverson, S. V., Haddock, T. L., Beal, J. & Densmore, D. M. CIDAR MoClo: Improved MoClo Assembly Standard and New E. coli Part Library Enable Rapid Combinatorial Design for Synthetic and Traditional Biology. *ACS Synth. Biol.* **5**, 99–103 (2016).
41. Halleran, A. D., Swaminathan, A. & Murray, R. M. Single Day Construction of Multigene Circuits with 3G Assembly. *ACS Synth. Biol.* **7**, 1477–1480 (2018).
42. Addgene: CIDAR MoClo Extension, Volume I. https://www.addgene.org/kits/murray-cidar-moclo-v1/.
43. Vaiana, C. A. *et al.* Characterizing chemical signaling between engineered “microbial sentinels” in porous microplates. *Mol Syst Biol* **18**, MSB202110785 (2022).

## Supplementary Files

This is a list of supplementary files associated with this preprint. Click to download.

- SupplementaryTable.xlsx
- StatisticalAnalysis.xlsx
- sentinelplantsupp.pdf